30 November 1998

PHYSICS LETTERS A

ELSEVIER

Physics Letters A 249 (1998) 191–198

A continuum model for the jumping sandbox

C.E. Garza-Hume [a,1], Pablo Padilla [a,2], Héctor D. Ceniceros [b]

[a] *IIMAS, UNAM, Circuito Escolar, Cd. Universitaria, México, D.F., Mexico*

[b] *Centro de Investigación en Computación, Instituto Politécnico Nacional, Unidad Profesional Adolfo López Mateos, Zacatenco, México, D.F. 07738, Mexico*

Received 1 April 1998; revised manuscript received 1 September 1998; accepted for publication 1 September 1998
Communicated by C.R. Doering

Abstract

We propose a continuum model for the motion of sand oscillating vertically. We derive a nonlinear parabolic equation with a nonlinearity corresponding to a bistable potential multiplied by a switching function. This is obtained by modifying the equation for a free surface and incorporating the thermodynamics of the interface. © 1998 Elsevier Science B.V.

Keywords: Granular material; Continuum model; Bistable potential; Capillarity; Free surface; Non-linear PDE

1. Introduction

Granular materials appear in many contexts and applications, such as mining, agriculture, construction and the pharmaceutical industry (see for instance Ref. [4] for a recent survey or Refs. [3,5] and references therein). Besides, they have also been the subject of much interest in connection with self-organized criticality [1].

Granular materials are large conglomerations of discrete macroscopic particles and have a very unusual behavior. However, under some circumstances, they exhibit solid-, liquid- or gas-like features. Much work has been done to understand these materials but a comprehensive theory is still lacking.

A relatively simple system that has been studied experimentally is the so-called *jumping sandbox* which consists of a layer of sand in a container which is oscillating vertically. In fact, a similar experiment was carried out with powder by Faraday in 1831 [9]. Despite its simplicity, this system exhibits very complicated dynamics. We mention that the same experiment has also been performed with a fluid instead of sand [12] and the fact that in both cases some common features are observed will be important in our analysis.

Some of the main properties of the system are already present in a simplified model, namely, a completely inelastic ball under the influence of gravity on a vibrating platform [14]. In the past few years Melo, Umbanhowar and Swinney [15–17] have performed a series of experiments with the above-mentioned *jumping sandbox*. They introduce dimensionless parameters N and $\Gamma = 4\pi^2 A f^2 g^{-1}$, the thickness of the layer and the acceleration amplitude respectively, where A is the displacement amplitude, f is the drive frequency and g the acceleration due to gravity. In the experiment Γ is varied, from small values up to large values and then back to small values. During this process, several spatial patterns oscillating at a fraction of the drive

[1] E-mail: clara@uxmym1.iimas.unam.mx.
[2] E-mail: pablo@uxmym1.iimas.unam.mx.

PII S0375-9601(98)00696-3

frequency are observed. When Γ is very small, the whole layer of sand oscillates together with the tray, as if it were a solid body. When Γ is increased, several transitions occur, where stripes appear and then bifurcate into hexagons or flat regions separated by kinks. Some other changes occur until finally a disordered state is reached when the frequency is larger than a certain critical value. The system exhibits hysteresis, that is, when the frequency corresponding to this disordered state is decreased, and it lies roughly in the region where previously squares or stripes were present, localized structures appear. These structures, called *oscillons* in Ref. [15], are stable circular peaks that oscillate at half the drive frequency. They weakly interact with each other forming small chains and tend to stay in the same place. When Γ decreases even further, the oscillons disappear and squares form again.

From the numerical point of view, treating the system as a set of interacting particles is complicated, since it involves counting collisions and solving a large number of equations. Also, one can expect the overall behavior of the system to be the consequence of net forces due to the collective effect of grains. For these reasons, we propose a continuum model leading to the equation

$$z_t - \epsilon^2 \Delta z + T(t+\phi)\, W'(z) = 0, \qquad (1)$$

where $z(x,t)$ represents the "effective" height of the sand above a reference level, $T(t+\phi)$ is an oscillating function related to the motion of the tray, with phase ϕ, ϵ is a small parameter and W is a double well potential (see Section 2 for the details of the derivation). Using this model equation in one and two dimensions we can reproduce qualitatively the behavior displayed by the system. In particular, we obtain two radically different pictures, namely, either we get oscillating patterns or we obtain oscillating localized structures (see Section 3 where the numerical results are presented). The fact that one or the other is obtained depends on the phase ϕ of T. Recently other models have been proposed to understand localized structures. Cerda, Melo and Rica [7] propose a mechanism due to two competing processes, a focusing effect and a diffusion effect. Tsimring and Aronson in Ref. [21] propose an amplitude equation for the parametric instability coupled to the mass conservation law. There are models for fluids by Edwards and Fauve in Ref. [8]. In Ref. [2] Barrio et al. propose a model for a "complex fluid" consisting of a suspension of large molecules.

2. Derivation of the model

First we consider the case of a fluid in a vibrating container. Depending on the fluid, various phenomena are observed [12]. For water and small amplitude oscillations, some regular structures emerge. These can be explained with the usual small amplitude approximations which lead to either a linear wave equation (standing waves) or the KdV equation (see Ref. [11, Ch. 5]) which accounts for solitons. However, as detergent is added to the water, under some circumstances, other localized structures appear that cannot be modeled by the previous equations. As discussed in Ref. [12], they behave differently from solitons in that they do not seem to interact with each other or do so only very weakly. They do not have a characteristic speed of propagation, rather they tend to stay at the same place. In the same work, it is shown that these localized structures are crucially linked to the system dissipation produced by the detergent (see Ref. [13, §63] where it is pointed out that adsorbed films increase dissipative effects.) On the other hand, an important characteristic of granular materials is their strong dissipativity and it is therefore natural to think that these localized structures might be produced by a similar physical mechanism in both cases. This also suggests the possibility of using a continuous medium model for the jumping sandbox. Besides, it is pointed out in Ref. [7] that it can be seen from experiment that the motion of sand particles is similar to that of a fluid particle in a standing surface wave.

The model proposed in Ref. [2] also suggests that this is a reasonable assumption. We would like to use the standard fluid dynamics approach to describe the motion of the interface of the sand. However, in deriving the equations of motion, the interface is considered to be sharp. For a granular material in motion though, it is not even clear what this interface is, and properties like local density, might strongly vary with position near the "surface". This is also the case for the experiment with water if the detergent can diffuse and therefore, cannot be assumed to form a thin film on the surface. It is therefore necessary to incorporate a detailed thermodynamic description of the interface.

The introduction of a suitable local free energy density $\Psi(z)$ leads to a density profile $\rho(z)$ which is consistent with an interface of non-zero thickness. This gives rise to the usual models of Ginzburg–Landau, Cahn–Hilliard, Van der Waals etc. (see Ref. [20, Section 3.1]) In the simplest version of the theory, $\Psi(z)$ has the following form,

$$\Psi(z) = -M[\rho(z)] + \tfrac{1}{2}m\rho'(z)^2, \tag{2}$$

where ρ' is the gradient $\mathrm{d}\rho/\mathrm{d}z$ and m is a coefficient independent of $\rho'(z)$ and higher order derivatives. $-M$ is W-shaped (double-well potential), has the dimensions of a free energy density and is the negative of an excess pressure.

It must be noted that by doing this, a characteristic length is introduced. This length corresponds to the region of transition between phases and replaces the previous sharp interface. If this region is small enough in comparison with the equilibrium height of the fluid, it is still meaningful to speak of the interface.

Now we can proceed with the derivation of Eq. (1). Recall that the equations of motion of an incompressible fluid in terms of the velocity potential ϕ are, in dimensionless form,

$$\Delta\phi = 0, \tag{3}$$

$$\phi_z = 0, \quad \text{on } z = 0, \tag{4}$$

$$\eta_t + \phi_x\eta_x + \phi_y\eta_y = \phi_z, \quad \text{on } z = 1+\eta, \tag{5}$$

$$\phi_t + \tfrac{1}{2}(\phi_x^2 + \phi_y^2 + \phi_z^2) + \eta - S\Delta\eta(1+\eta_x^2+\eta_y^2)^{3/2} = 0, \quad \text{on } z = 1+\eta. \tag{6}$$

Here the bottom is at $z = 0$ and Eq. (4) means that the vertical component of the velocity is zero there. The equilibrium height is $z = 1$ and $\eta = z - 1$ represents the deviation of the surface from it. Eq. (5) follows from the fact that the fluid elements on the surface remain part of the main body of the fluid. Finally, Eq. (6) follows from pressure balance on the surface. In this equation S is a dimensionless constant related to the surface tension T, acceleration of gravity g, density of the fluid ρ and the equilibrium height, h,

$$S = \frac{T}{g\rho h^2}$$

(see Ref. [11, pp. 14, 100] for further details). We will take this set of equations as starting point and will make several approximations and modifications. First, since the motion we describe is due to a vertical forcing we will only take vertical displacements on the surface, that is, ϕ_x and $\phi_y = 0$. We assume that except for a very small region near the surface, the material is incompressible, and therefore, in the bulk of the material, away from the free boundary, the density is constant. This is certainly the case for water and detergent. Next, in Eq. (6), we neglect the term ϕ_t. From the discussion above, both for sand and water with detergent, very strong dissipative effects near the surface are to be expected. If we take into account this fact, a term proportional to the Laplacian of ϕ should be added, just as for the Navier–Stokes equation. Presumably, the system will arrive at a stationary state very rapidly, making the term ϕ_t small. Then, the system simplifies to

$$\Delta\phi = 0, \tag{7}$$

$$\phi_z = 0, \quad \text{on } z = 0, \tag{8}$$

$$\eta_t = \phi_z, \quad \text{on } z = 1+\eta, \tag{9}$$

$$\tfrac{1}{2}\phi_z^2 + \eta - S\Delta\eta(1+\eta_x^2+\eta_y^2)^{3/2} = 0, \quad \text{on } z = 1+\eta. \tag{10}$$

Now the term in Eq. (10) which is multiplied by S, comes from considering the interface as an elastic membrane and can be obtained computing the first variation of the corresponding potential energy. If we want to take into account that the interface has some structure, we can proceed by replacing this energy with (2). This is given in terms of the density ρ, and we would like to express it in terms of z. In order to do this, we notice that the dependence of z in terms of ρ can be obtained explicitly (see Ref. [20, p. 55, Eq. (3.9)]). The form of $-M$ as a function of z is qualitatively the same, since ρ turns out to be a monotone function of z, and we will denote it by W. As pointed out in the same reference, this potential energy is a good approximation when ρ is slowly varying, so we will replace the term involving $(\rho')^2$ by $D|\nabla z(x,y)|^2$, where D is a small constant. Then Eq. (10) becomes

$$\tfrac{1}{2}\phi_z^2 + z - 1 - D\Delta z + W(z) = 0.$$

Solving for ϕ_z and approximating

$$\sqrt{v} \simeq \frac{v}{\sqrt{v_0}},$$

for $0 \leqslant v \leqslant v_0$ (that is, approximating the square root in this interval by the segment joining 0 and $(v_0, \sqrt{v_0})$, and substituting into Eq. (10) we obtain

$$z_t = \varepsilon^2 \Delta z + TW(z) + B(z-1),$$

with ε, T and B constants. So far, we have not taken into account that the bottom is oscillating. We suppose that the *net* effect of this oscillation is to modify the value of gravity by introducing a periodic variation on g. Again, this is consistent with Ref. [2]. In terms of the potential W, this would have the effect of changing the stability of its critical points, at least for some time during the oscillation and suitable amplitudes. The easiest way to achieve this is to have T change sign. So T becomes a periodic function. Observe that this does not contradict the fact that we have already neglected the ϕ_t term, for we are only interested in the *effective* motion of the surface and so we do not consider the changes in this term during small time intervals. This is similar to the usual multiple time scale analysis when obtaining effective equations for the envelope of a wave packet [11]. In any case, its range of validity depends on the frequency of the oscillatory motion. By doing this, we finally obtain Eq. (1). Actually Eqs. (7)–(10) are written with respect to the floor and not the bottom of the tray and strictly speaking one would have to take into account the oscillation of the tray in the coordinate system used, but if the oscillation has small amplitude this can be ignored.

In the remainder of this section we discuss why the previous equation gives rise to both periodic patterns and localized structures. Recall that from the experimental results two different types of structures appear, one that we simply call "patterns", which corresponds to the formation of interfaces, squares and hexagons and another one, that has been designated as "*oscillons*", which is a localized structure exhibiting some periodic behavior.

From the mathematical point of view, the description of pattern formation in different situations has been very much studied (see for example Refs. [10,18]). In many of these models a common feature is the use of a bistable potential as the first and simplest approximation (Ginzburg–Landau, Cahn–Hilliard, etc.).

That some kind of bistability might be the underlying mechanism generating some specific structures is suggested by the dissipative nature of sand. A prototypical equation for these processes is

$$\frac{\partial u}{\partial t} - \epsilon^2 \Delta u + W'(u) = 0, \quad \text{in } \Omega,$$
$$\frac{\partial u}{\partial \nu} = 0, \qquad \text{on } \partial\Omega,$$

where u is the state variable. In our case $u(x)$ represents the height of the sand surface above some reference level and W is a local potential energy density. We also observe that equilibrium (time independent) solutions of (11) correspond to critical points of the energy

$$E(u) = \int_\Omega \left(\tfrac{1}{2}\epsilon |\nabla u|^2 + \frac{1}{\epsilon} W(u) \right) \mathrm{d}x.$$

When ϵ is small, in order for the energy to remain bounded, $u(x)$ has to stay very close to the zeros of W and the transitions separating these two values give rise to the formation of patterns.

On the other hand, equations that show solutions localized in very small regions have also been considered in many contexts. We mention the work by Ni and Takagi in Ref. [19] as a fundamental reference, but we should point out that much work has been done on the subject. They consider the equation

$$\frac{\partial u}{\partial t} - \epsilon^2 \Delta u + M'(u) = 0, \quad \text{in } \Omega,$$
$$\frac{\partial u}{\partial \nu} = 0, \qquad \text{on } \partial\Omega,$$

where $M(u) = -W(u)$. For this equation, initial conditions that take large positive and negative values will tend to develop peaks (see Fig. 4). Notice that the corresponding energy for stationary solutions

$$E(u) = \int_\Omega \left(\tfrac{1}{2}\epsilon |\nabla u|^2 - \frac{1}{\epsilon} W(u) \right) \mathrm{d}x$$

is not bounded from below. Eq. (1) is then obtained by combining these two dynamics by means of a switching function $T(t+\phi)$, τ-periodic. If T is oscillating between -1 and 1, that is, when

$$T(t) = -1, \quad \text{if } -\tfrac{1}{2}\tau < t < 0,$$
$$= 1, \quad \text{if } 0 < t < \tfrac{1}{2}\tau,$$

we have the dynamics corresponding to (11) for half of the period and that of (12) for the other half.

In our model then, the pattern formation process takes place during the second half and oscillons are formed in the first half. In fact, for this case, it is easy to paste solutions of (11) and a trivial solution, zero, for our W or correspondingly solutions to (12) and zero to obtain solutions of (1) discontinuous in time that exhibit oscillating patterns and oscillating peaks respectively.

The fact that Eqs. (11) and (12) exhibit the features that we have mentioned can also be visualized by considering the ODE analogues

$$\dot{x} = -\frac{W'(x)}{\epsilon},$$

$$\dot{x} = -\frac{M'(x)}{\epsilon} = \frac{W'(x)}{\epsilon}.$$

The corresponding numerical solutions are shown in the next section.

3. Numerics

In this section we present several numerical experiments that validate our model as well as some details on the numerical methods used to solve the equations.

Some numerical solutions of the ODEs are shown in Figs. 1 and 2. Fig. 1 shows the trajectories for the ordinary differential equation with W-shaped potential energy. Zero is an unstable solution, 1 and -1 are stable solutions. Trajectories that start above zero tend to 1 and those that start below zero tend to -1. In Fig. 2 we show trajectories for the ODE with M-shaped energy and therefore solutions that start between -1 and 1 tend to 0 which is now the stable solution and others go to plus or minus infinity.

For the partial differential equation in one space dimension, when the energy is a "W" we observe patterns, i.e. flat regions separated by sharp transitions (Fig. 3); when it is an "M" we observe the formation of a peak (Fig. 4). In the presence of the switching term, depending on the phase, we observe localized

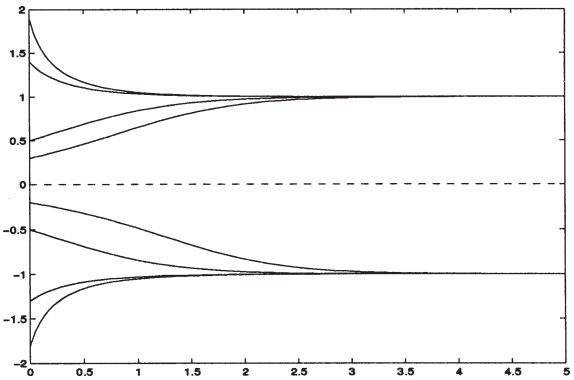

Fig. 1. Trajectories for the ODE with W-shaped energy.

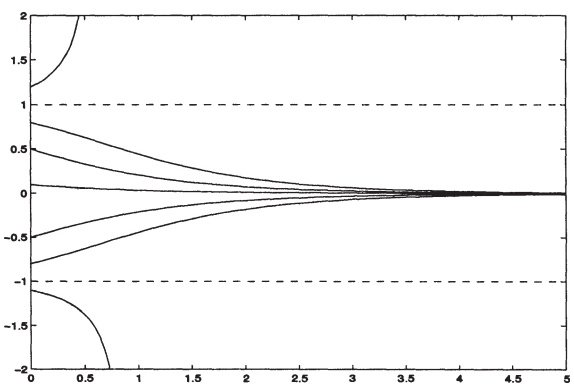

Fig. 2. Trajectories for the ODE with M-shaped energy.

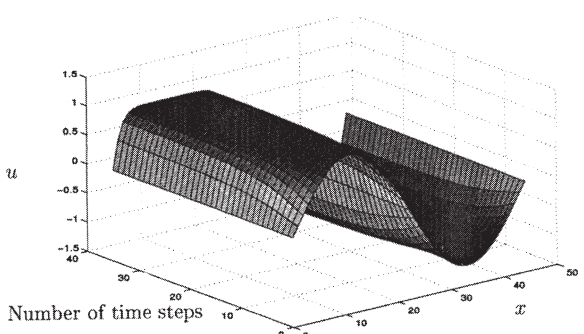

Fig. 3. Initial condition $1.1\sin(2\pi\alpha x)$. Energy is "W", the region between $+1$ and -1 becomes narrower with time.

solutions that persist for some cycles (Figs. 5–7) or patterns (Fig. 8).

Next we show the figures obtained in two space dimensions. With the same initial condition shown in Fig. 9, depending on the phase of the switching function we observe oscillons as in Fig. 10 or patterns as

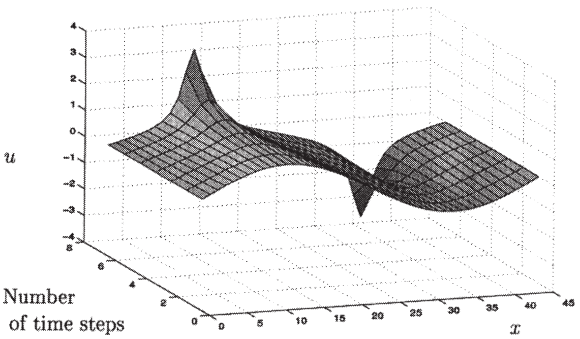

Fig. 4. Energy is an "M", peak develops.

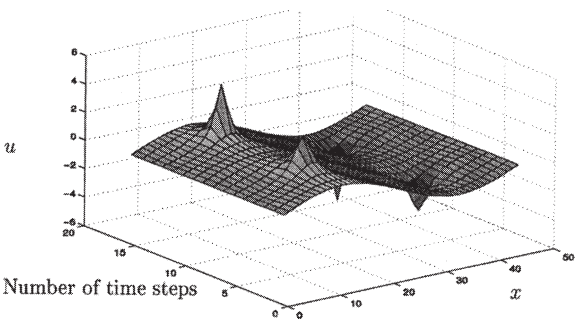

Fig. 5. Equation with switching function. Peaks develop.

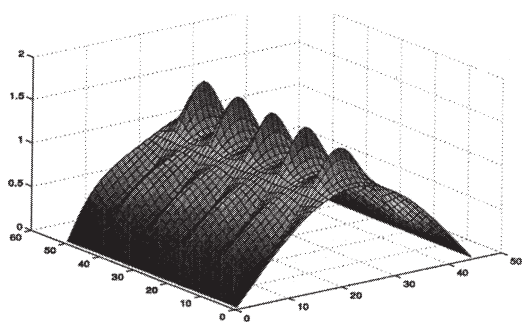

Fig. 6. Equation with switching function. Peaks form.

in Figs. 11, 12 and 13. Note that the last three figures correspond to different times with the same initial condition and phase.

3.1. The numerical method

To solve the partial differential equation (1) in $\mathbb{R}$ we use a standard subroutine that can handle equations of the form

$$u_t = f(x, t, u, u_x, u_{xx}).$$

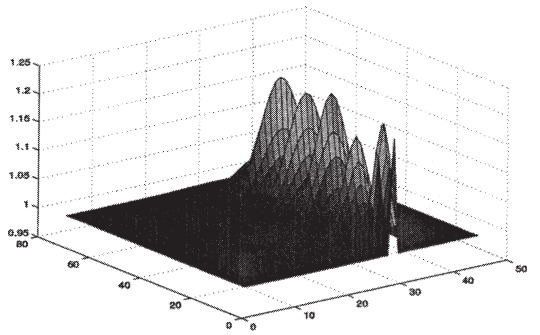

Fig. 7. Equation with switching function. Peaks form.

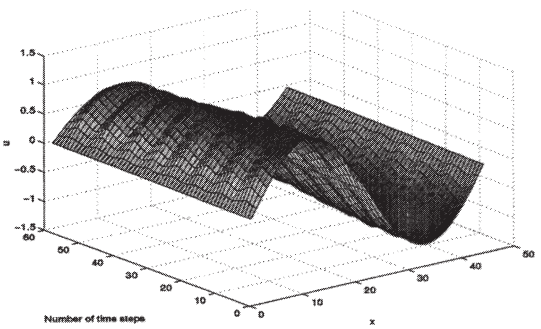

Fig. 8. Equation with switching function of opposite phase.

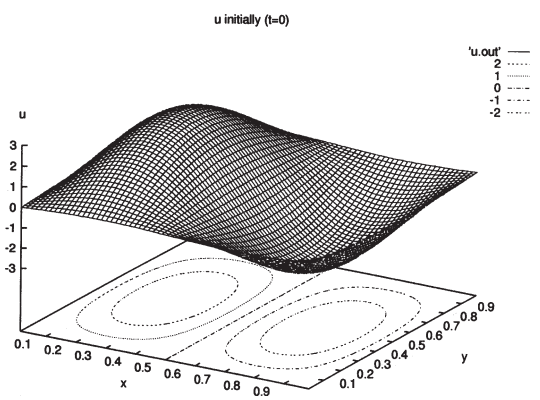

Fig. 9. Initial condition.

It uses the method of lines and represents the solution using cubic Hermite polynomials.

In $\mathbb{R}^2$ we use Crank–Nicholson plus the method of conjugate gradients. The equation we have in $\mathbb{R}$ is

$$u_t = \epsilon u_{xx} - \frac{D}{\epsilon}(u^3 - u),$$

where D is an oscillating function. One of the functions we use is

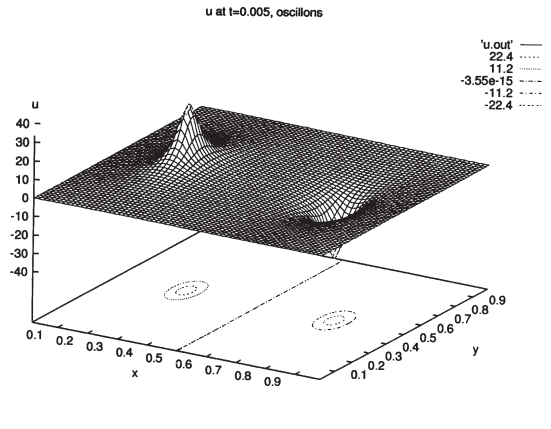

Fig. 10. 2D, "oscillons".

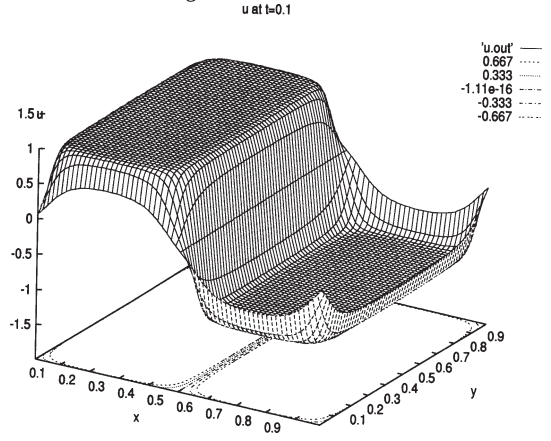

Fig. 11. 2D, interfaces.

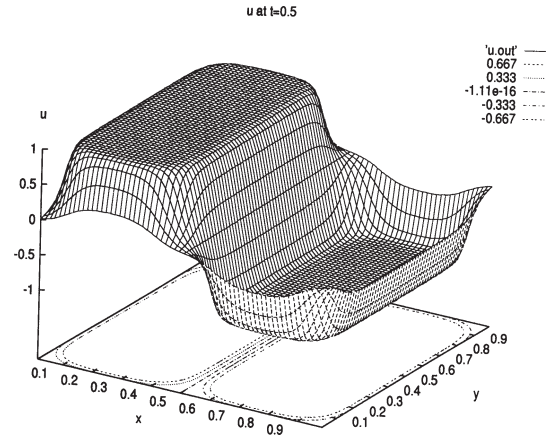

Fig. 12. 2D, interfaces.

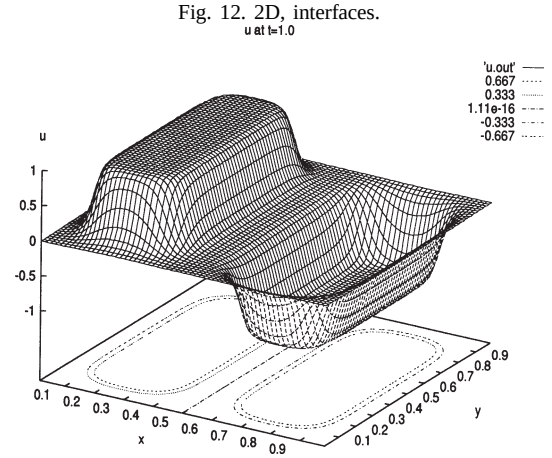

Fig. 13. 2D, interfaces.

$$D = +1, \quad \text{if } \sin(2\pi t\alpha) \geqslant \beta,$$
$$= -1, \quad \text{otherwise,}$$

where α and β are constants. In Figs. 4–7, $\alpha = 24.5$ and β is between 0.1 and 0.2. In the examples shown $\epsilon = 0.03$. The step-size was in most cases 0.004.

Acknowledgement

We would like to thank Jose Luis Lopez Gonzalez for mentioning the problem to one of the authors.

References

[1] P. Bak, How Nature Works (Oxford Univ. Press, Oxford).
[2] R. Barrio, J.L. Aragón, C. Varea, M. Torres, I. Jiménez, F. Montero de Espinosa, Robust symmetric patterns in the Faraday experiment, Phys. Rev. E 56 (1997).
[3] H.M. Jaeger, S.R. Nagel, R.P. Behringer, Phys. Today 49 (1996) 32–38.
[4] H.M. Jaeger, S.R. Nagel, R.P. Behringer Granular solids, liquids and gases, Rev. Mod. Phys. 68 (1996).
[5] G. Capriz, Mullenger, Extended continuum mechanics for the study of granular flows. Rend. Acc. Lincei, Matematica.
[6] G. Capriz, Mullenger, Critical modelling aspects: Granular flows, layering in smectics, in: Continuum Models and Discrete Systems, Proc. of the Eighth Int. Symp., ed. K. Markov (World Scientific, Singapore, 1996).
[7] Cerda, Melo, Rica, Model for subharmonic waves in granular materials, Phys. Rev. Lett. 79 (1997).
[8] Edwards, Fauve, J. Fluid Mech. 278 (1994) 123–148.
[9] M. Faraday, Phil. Trans. R. Soc. London, 52 (1831) 299.
[10] U. Grenander, General Pattern Theory, Oxford Mathematical Monographs (Clarendon, Oxford, 1993).
[11] E. Infeld, G. Rowlands, Nonlinear Waves, Solitons and Chaos (Cambridge Univ. Press, Cambridge, 1990).

[12] O. Lioubashevski, H. Arbell, J. Fineberg, Dissipative solitary states in driven surface waves, Phys. Rev. Let. 76 (1996).
[13] Landau, Lifschitz, Fluid Mechanics, Course of Theoretical Physics Vol. 6 (Pergamon, New York, 1987).
[14] A. Metha, J.M. Luck, Novel temporal behavior of a nonlinear system: The completely inelastic bouncing ball, Phys. Rev. Lett. 65 (1990) 393.
[15] F. Melo, P.B. Umbanhowar, H.L. Swinney, Oscillons observed, Nature 382 (1996) 6594.
[16] F. Melo, P.B. Umbanhowar, H.L. Swinney, Hexagons, kinks, and disorder in oscillated granular layers, Phys. Rev. Lett. 75 (1995) 3838.
[17] F. Melo, P.B. Umbanhowar, H.L. Swinney, Transition to parametric wave patterns in a vertically oscillated granular layer, Phys. Rev. Lett. 72 (1994) 172.
[18] A. Newell, T. Passot, J. Lega, Order parameter equations for patterns, Ann. Rev. Fluid Mech. 35 (1993) 399–453.
[19] W.M. Ni, I. Takagi, On the shape of least-energy solutions to a semilinear Neumann problem, Comm. Pure Appl. Math., 46 (1991) 819–851.
[20] J.S. Rowlinson, B. Widom, Molecular Theory of Capillarity (Clarendon, Oxford, 1982).
[21] L. Tsimring, I. Aronson, Localized and cellular patterns in a vibrated granular layer, Phys. Rev. Lett. 79 (1997).